Investigation of the Moisture Buffering Potential of Magnesium Oxide Board

Submitted to:

Peter Francis, President

MAGO Building Products Ltd

201 33 East 8th Ave | Vancouver, BC, V5T 1R5

April, 2016

Prepared by:

Fitsum Tariku, Ph.D., Principal Investigator

Barilelo Nghana, MEng, Researcher Analyst

Building Science Centre of Excellence

British Columbia Institute of Technology

3700 Willingdon Avenue

Burnaby, British Columbia, V5G 3H2

Acknowledgements

EXECUTIVE SUMMARY

Passive humidity control in buildings can be achieved by incorporating materials with moisture buffering potential in that these materials absorb moisture at peak times and give off the stored up moisture at low moisture production times thereby stabilizing the interior relative humidity. Some of the advantages of this phenomenon include but are not limited to energy savings, improvement of thermal comfort and perceived air quality. As such, it is necessary to investigate different materials for their moisture buffering capabilities. As part of product development, the moisture buffering characteristics of Magnesium oxide board (Magnesia board) is experimentally investigated. Other considerations such as the impact of surface finishing and ventilation are also assessed. The experiment is done by monitoring twin buildings termed the Whole Building Performance Research Laboratory (WBPRL) while measuring the relative humidity evolution in time. One is set as the reference building and finished with gypsum wallboard owing to its wide industry use. The other is set as the reference building and covered with the Magnesia board. Both buildings are first validated under non-hygroscopic conditions to ensure similar hygrothermal loading and operation of both buildings. Next, four tests are conducted to simulate surface treatments, ventilation effects, and occupancy density. For each test run, four cases are created for different surface treatment configurations. From the test, it is found that magnesia board and gypsum demonstrate similar moisture buffering characteristics. In the as-in service case where the gypsum wallboard is painted with latex paint, as it is the current common practice, and magnesia board with the company specified paint, the later demonstrates slightly better moisture buffering due to the high permeability surface treatment.

Table of Contents

1 INTRODUCTION

One of the main factors responsible for building envelope failures is excess humidity in that hot humid air condenses on a cold surface when in contact. Additionally, the presence of excess humidity creates a favorable environment for mold growth on the interior finish of the building envelope. The respiratory health risks associated with the presence of mold in the indoor environment is well documented, therefore stressing the need for humidity control within an acceptable range. To further emphasize the necessity for humidity control, of the most important environmental parameters necessary for mold growth on a building material; temperature and relative humidity or moisture [1-4], relative humidity control is more feasible since mold thrives in temperatures within the human comfort range. Indoor humidity control is most commonly achieved by ventilation [5-8]. However, providing excess ventilation beyond code requirements to control indoor humidity negatively impacts the energy performance of the building since the outdoor air is typically conditioned to near comfort conditions. A passive means of controlling indoor humidity is therefore necessary to reduce the ventilation energy requirements. Passive indoor humidity control can be achieved by employing interior finishes with moisture buffering capacity [9-21]. Such materials absorb moisture at high humidity levels and release the moisture back to the indoor space when the indoor humidity is low. As such, the ventilation required, especially at peak moisture production conditions is minimized. Consequently, the ventilation energy consumption of the building is reduced [29]. Additional consequences of this moisture buffering phenomenon are improvement of comfort and perceived air quality [12, 16, 19, 25], reduction of heating energy [16, 19, 22, 27, 30], reduction of cooling energy [19, 22, 30], reduction of humidification and dehumidification energy demand [23, 24, 25], reduction of the building's latent heat load [26, 28]. Owing to the advantages of this moisture buffering effect, many materials

are being investigated for their moisture buffering capacity [31, 32]. In this project, a relatively new material called Magnesium oxide board; also referred to as Magnesia, is experimentally investigated for its ability to modulate interior relative humidity in a mild climate like Vancouver, BC.

2 RESEARCH METHODOLOGY

2.1 Scope

The aim of this study is to investigate the moisture buffering potential of Magnesia boards. This involved monitoring two identical side-by-side buildings under different operation scenarios while measuring the indoor air temperature and relative humidity. The aforementioned variables are analyzed to evaluate the moisture buffering relative to the baseline material. These two buildings are termed the Whole-Building Performance Research Laboratory; a state-of-the-art test facility, located in an open area on the BCIT Burnaby campus such that building structures or terrestrial bodies do not interfere with the external climate [33]. One of the two buildings is designated the 'reference building' and the second one, the 'test building'. The interior of the 'reference building' is finished with gypsum panels, which is indicative of typical industry choice of interior finishing material, and the 'test building' is finished with the Magnesia board. The two buildings are exposed to similar outdoor climatic conditions and indoor hygrothermal loads. The indoor hygrothermal loads are defined to reflect realistic building loading which is indicative of a typical residential family building occupancy variation and the activities associated with their heat and moisture generation rates. Specifically, average and high occupancy density cases are considered and the corresponding daily heat and moisture generation profiles are developed and implemented in both buildings using the already in-house developed occupant simulators. These occupancy simulators have the potential to simulate heat generation, CO_2 generation and moisture; however, in this

project only the moisture generation is simulated. Other variables considered, besides the occupancy density are effect of finishing, ventilation rate, ventilation control strategy and a combination.

2.2 Methodology

The moisture buffering potential of magnesia board is experimentally analyzed. As stated earlier, the derived indoor hygrothermal loading is generated by the in-house built occupancy simulators. As such, these occupancy simulators are first calibrated in the laboratory to determine the moisture output of the system into the ambient. Secondly, the laboratory calibrated moisture generation rate is verified in the field under actual test conditions. This is to ensure that the derived indoor hygrothermal loading profile is accurately being simulated in both buildings such that the moisture output is accurate and the humidity levels in the two test buildings are identical. It should be noted that in this phase of the experiment, all other sources of moisture are eliminated by lining the interior of both test facilities with 6 mil polyethylene film. Upon field verification of the occupancy simulator output, the moisture buffering potential of the magnesia board is investigated under different operating conditions. The four conditions are: normal moisture production at 15cfm ventilation rate, high moisture production (i.e. 1.5x the normal production rate) and 15cfm ventilation rate, normal moisture production and 7.5cfm ventilation rate, and normal moisture production and relative humidity controlled ventilation so as to maintain the interior relative humidity between 50% and 60%. More detail on the reasoning behind each test construction is given in the test run sub-section under the field testing section. The details of the experimental setup and procedure are presented in the accompanying sections.

# 3 CALIBRATION OF THE OCCUPANCY SIMULATOR SYSTEMS

3.1 Overview
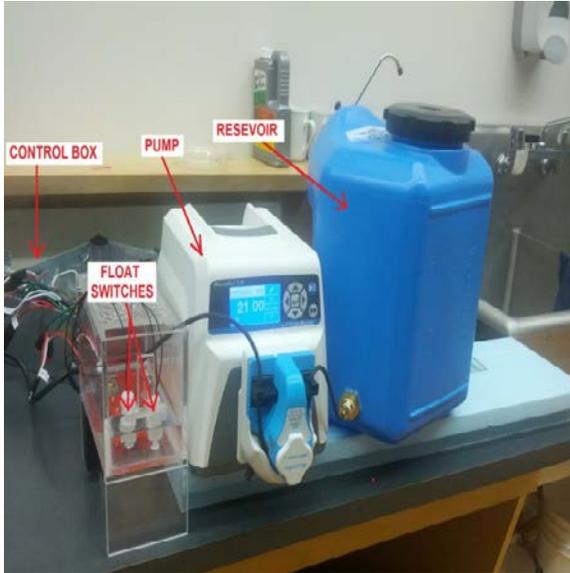
Figure 1 - Humidification System Components of the occupant simulator system [34]
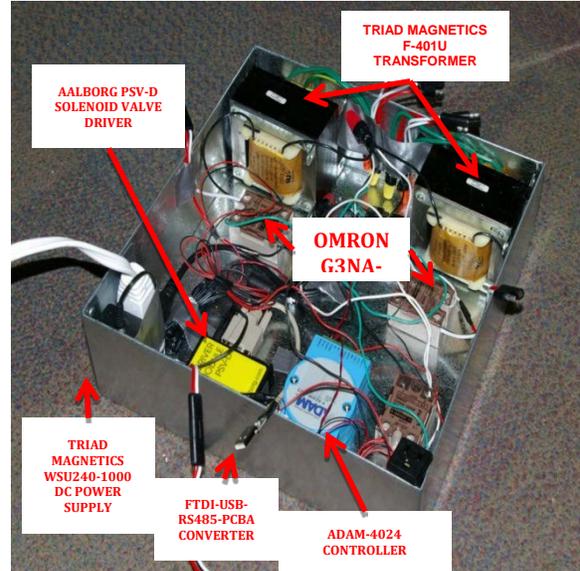
Figure 2 - Control Box Major Components

3.1.1 Description of humidification System

The humidification system is part of a system called the indoor simulation system that is designed to simulate household daily activities including moisture, heat and CO_2 generation. The other components of this indoor simulation system are a control box for power supply and control, a lamp for heat generation and a CO_2 tank with solenoid valve for CO_2 generation. The humidification system consists of two humidifier boxes, two digital pumps, and two water reservoirs. The humidifier boxes consist of the nebulizers, a fan and two float sensors. All three components coordinate such that the nebulizers evaporate the water and the fan acts to blow the water vapor into the space. As well, the two float sensors; a water level float sensor and safety float sensor, act to maintain the water level in the humidifier boxes by communicating with the digital pumps and maintain safe operation of the nebulizers in the event of leakage of the

4

humidifier box or shortage of water in the water reservoirs. Figure 1 shows the components of the humidification system. The operational flexibility of the humidification system is achieved by a Vee program that communicates with the Adam controller to open or close the relay switches. The duration of the relay switch states is based upon the hourly moisture production requirement. Figure 2 highlights the major components of the control box. Given that the duration of the relay switch ON and OFF times is based in the moisture production, each occupancy simulator unit needed to first be calibrated to ensure accurate prediction of the inputs for the Vee program.

3.2 Calibration Procedure

The aim of this calibration is to determine the evaporation rate of the individual humidifier boxes. The secondary objective of the calibration is to verify manufacturer specified misting rate of the nebulizers. To calibrate the nebulizers, the humidifier boxes are allocated to an indoor simulation control box and labelled accordingly to maintain consistency and balance out the operation time of the nebulizers during operation such that a sufficient nebulizer cooling time is allowed. Following, the humidification system is assembled, leveled and connected to the control box as labelled. Upon, labeling and assembly of the indoor simulation system, a trial run is performed to determine the water level at which the pump is triggered to begin refill of the humidifier box. This point is marked and a 2cm band is created such that the marked point is situated within this band. The pump trigger water level is of interest because this is the level the water will be maintained at in the field experiment. The pump is then disconnected from the humidification system since the pump refill action is simulated manually from here on. The humidification box is then filled with water to the upper limit of the band earlier created and placed on a weighing scale that is connected to a computer for data acquisition (Figure 3). The weighing scale keeps track of the dynamic weight changes over the course of the experimental period. The data acquisition from the weighing

scale is by means of a Vee program that extracts data every 10 seconds. Once setup is complete, the nebulizer is run continuously for a period of 1 hour while maintaining the water level between the upper limit and lower limit of the band earlier created. Each humidifier box is calibrated 3 times with data extracted and analyzed.
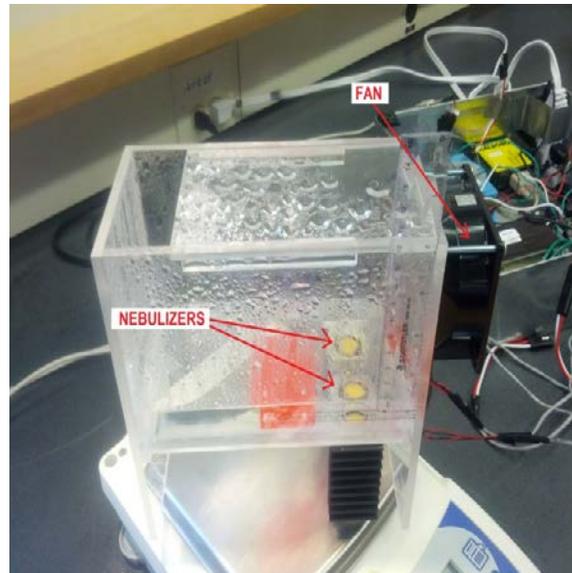
Figure 3 - Laboratory setup for calibration of the indoor simulation units[34]

3.3 Calibration Results

From the data recorded during the calibration experiment, the weight loss per data collection interval is calculated and evaluated to indicate the cumulative weight loss. From this an excel plot is created representing the cumulative weight loss over time. A linear fit is imposed on the data points per 15 minutes such that the slopes of the linear fits depict the moisture production rate of each humidifier box. The slopes of the linear fit are then averaged ignoring the first quarter, since it is regarded as the start-up phase and it is anticipated that this phase may introduce uncertainties in the results. It should be noted that the simulation of the pump refill action by refilling the

humidifier box introduces some irregularities in the data. This is accounted for by zeroing all negative weight loss calculated from the time before.

Four humidifier boxes are calibrated, namely: 1111, 2221, 3112, and 4222. The naming nomenclature is as follows, the 1st digit signifies an arbitrarily chosen number, and the 2nd matches the number tag on the control box. Each control box has the capacity to operate two humidification boxes. As such, all the channels and wire connections are labeled "1" or "2" to prevent mismatching, the 3rd digit is the number of nebulizers in each humidifier box; some boxes have more than one nebulizers to increase the misting rate, and the 4th digit is the control box tag; since there are two control boxes; one for each building, both and labeled "system 1" and "system 2". For brevity only the calibration of box 1111 is presented in detail; however, the same procedure is followed for all the other boxes.

Figure 4, Figure 5 and Figure 6 show the linear plot for three calibration runs for box 1111. One can immediately notice the plateaus in the plot. In some cases, they are pronounced than the others, these plateaus coincide with the water refilling of the humidifier boxes while in operation. Recall, these points yielded negative weight change over the data acquisition interval, hence, when zeroed, yielded constant cumulative weigh loss over the period. More important is the slope of the quarterly linear fits for the different runs which signify the evaporation rate of the humidifier box. The evaporation rate is close to within 9%. This attests to the consistency and reliability of the nebulizers. Based on the evaporation rate derived in 2nd, 3rd and 4th quarter of all three runs, the evaporation rate of box 1111 is 90 g/hr.
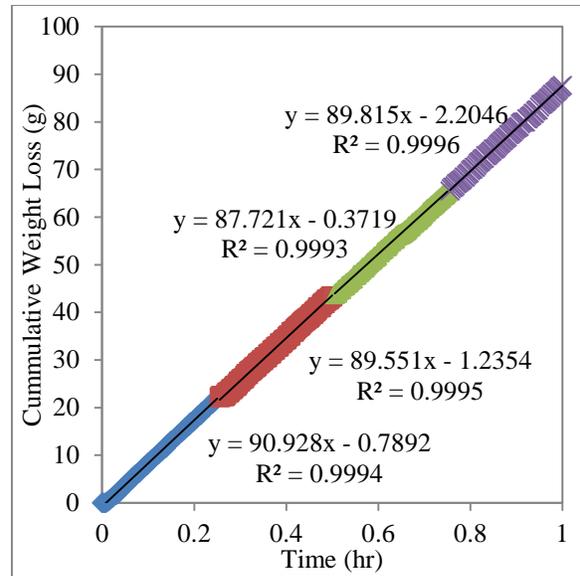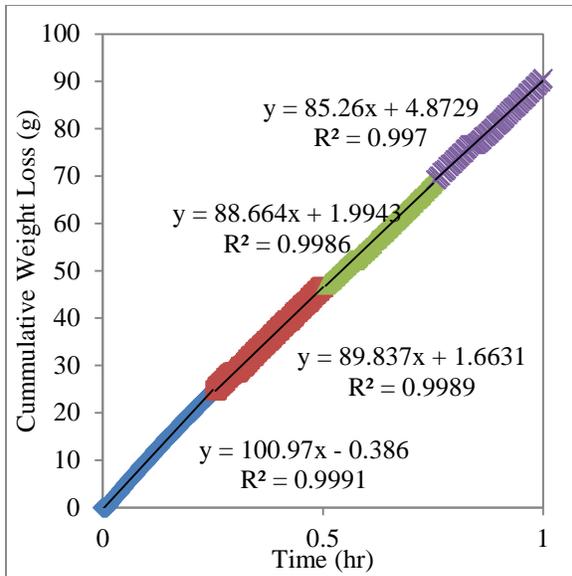
Figure 4 - Calibration of box 1111: Run #1

Figure 5 - Calibration of box 1111: Run #2
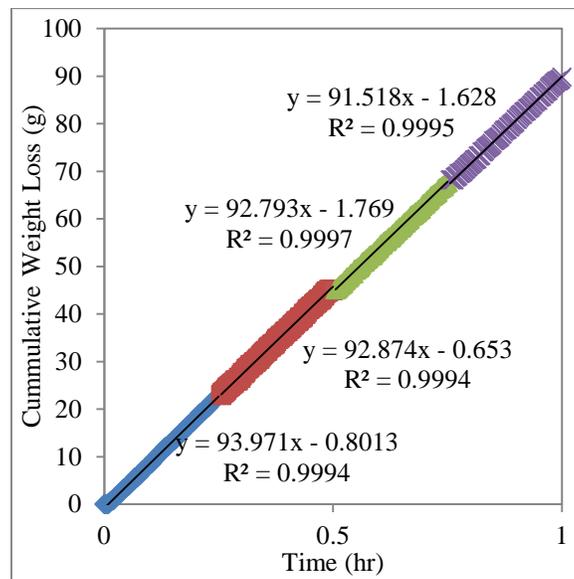
Figure 6 - Calibration of box 1111: Run #3

It should be noted that while averaging the slopes of the linear fits, the slopes of the first quarter for each run is not considered, this is because it is believed that the system is not fully stabilized in that the misting action of the nebulizer causes water droplets to adhere to the surface of the humidifier box. When the surface of the humidifier box can no longer hold more of these water

droplets they begin to drain back into the pool of water in the humidifier box. This is more pronounced in the first run than the others because initially the walls of the humidifier box are void of water which prolongs the time taken for the system to stabilize. On the other hand, the second and third run are carried out successively which implies that some moisture is already deposited on the walls of the humidifier boxes ensuring a shorter time required to reach steady state operation. This is evident in the smaller deviation of the evaporation rate of the initial quarter from the steady state values. The same data analysis procedure is carried out for box 2221, 3112 and 4222 and an evaporation rate of 141 g/hr, 70 g/hr and 126 g/hr is derived respectively.

4 VERIFICATION OF THE DERIVED EVAPORATION RATE IN ACTUAL TEST CONDITIONS

The second phase of the calibration is carried out in the WBPRL. The aim of this calibration is to verify the moisture production rate of the humidifier boxes determined from the calibration procedure and to ensure that both test facilities are operating at the same conditions. A brief overview of the test facility is provided in this section, followed by the experimental setup of each test facility. The results are presented thereafter.

4.1 Overview of the test facility

4.1.1 Construction

Figure 7 - From left: North and South Test-hut [33]

Two identical test building facilities located in BCIT, Burnaby campus (123° Longitude and 45° latitude) are monitored to assess the moisture buffering effect of two materials. The two buildings are designated names consistent with their relative position on the site; North and south building (Figure 7), with length, width, and height dimension as 16' x 12' x 8'. The buildings are positioned such that the surrounding buildings and terrestrial bodies do not interfere with the external climate. The two buildings have HSS steel skeleton-frame structure and insulated slab on grade foundation with the exterior walls and roofs constructed with 2" x 6" studs 16" O.C and 2" x 12" wood joists

and rafters respectively. Table 1 shows a complete description of the wall, roof and floor assembly. Both buildings have two windows in the north and south wall orientation. The windows are vinyl framed and air filled with height and width dimensions of 4' x 3' respectively. As well, some of the floor area is take up by the mechanical room in both buildings. The mechanical room houses the air handling unit, data acquisition systems and instrumentation. The mechanical room is separated from the interior space by an interior partition (Table 1) with doors linking the exterior and the interior space. The doors are fabricated of metal with a hollow core. The height and width dimensions of the doors are 8' x 4'. The North and South buildings are air tight according to ASHRAE's (2013) buildings' air tightness classification having effective leakage areas of 25cm^2 and 29cm^2 respectively [33].

Table 1 - Envelope Construction Details

Component	Assembly detail	
wall	Exterior Wall	Interior Wall
	5/6" fiber cement cladding ¾" air cavity - SBPO ½" Plywood sheathing board 2" x 6" Wood stud w/ R20 fiberglass batt insulation 6mil Polyethylene film ½" gypsum drywall	½" Plywood sheathing board 2" x 4" Wood stud w/ R14 fiberglass batt insulation ½" Plywood sheathing board ½" gypsum drywall
Roof	2 ply SBS modified bitumen	

	• Plywood sheathing	
	• Air gap	
	• 2" x 12" wood joist w/ R40 glass fiber insulation	
	• 6 mil polyethylene sheet	
	• drywall	
Floor	• 12" concrete slab	
	• 3" Rigid Insulation	
	• 6 mil Polyethylene film	

4.1.2 Mechanical Equipment

The WBPRL is equipped with a highly flexible mechanical system composed of two major systems; air flow and air conditioning system. The air flow system is responsible for controlling and delivering required ventilation rates with an added feature to implement demand control ventilation. The air conditioning unit, as the name implies, is responsible for adjusting the temperature and humidity of the supply air to the appropriate states. Both systems combine to provide heating, cooling, ventilation, humidification, and dehumidification.

4.1.3 Weather Data

The outdoor climatic conditions to which the buildings are exposed to, including temperature, relative humidity, wind speed and directions, solar radiation and rain loads, are measured by an onsite weather station (Figure 8).

Figure 8 - Weather Station

4.2 Experimental Setup

4.2.1 Installation of the Polyethylene

To eliminate other sources of moisture besides that generated by the humidification system, the interior surfaces of the walls, ceiling and floor are lined with 6 mil polyethylene sheets. These sheets are overlapped 6" at its ends and taped securely to ensure continuity and vapor tightness of both facilities (Figure 9).

4.2.2 Instrumentation

For data collection, both buildings are fitted with relative humidity and temperature (RH-T) sensors (L: 71mm, D: 12mm, accuracy: $\pm 0.6^{\circ}$C $\pm 3\%$) at various levels to measure the zone air temperature and relative humidity as the name suggests. The RH-T's are positioned to account for thermal stratification and location of window openings. The RH-Ts are positioned at three locations in both buildings. One closest to the air supply inlet, the other farthest from the air supply inlet and three at the middle of the room. The three at the middle of the room are layered at about

2ft, 5ft and 7.7ft above the ground. The one closest to the air supply is 5ft from the base such that is not affected by the sudden opening and closing of the door. The one farthest from the supply inlet is 2ft from the ground and is positioned such that the solar radiation from the window does not affect the readings of the RH-T. The Data is extracted from the RH-T sensors by means of a data acquisition system that is configured to collect data within 5 min intervals. The data collected is stored on site and can be retrieved easily. Data from the weather station is collected per 1 minute interval.
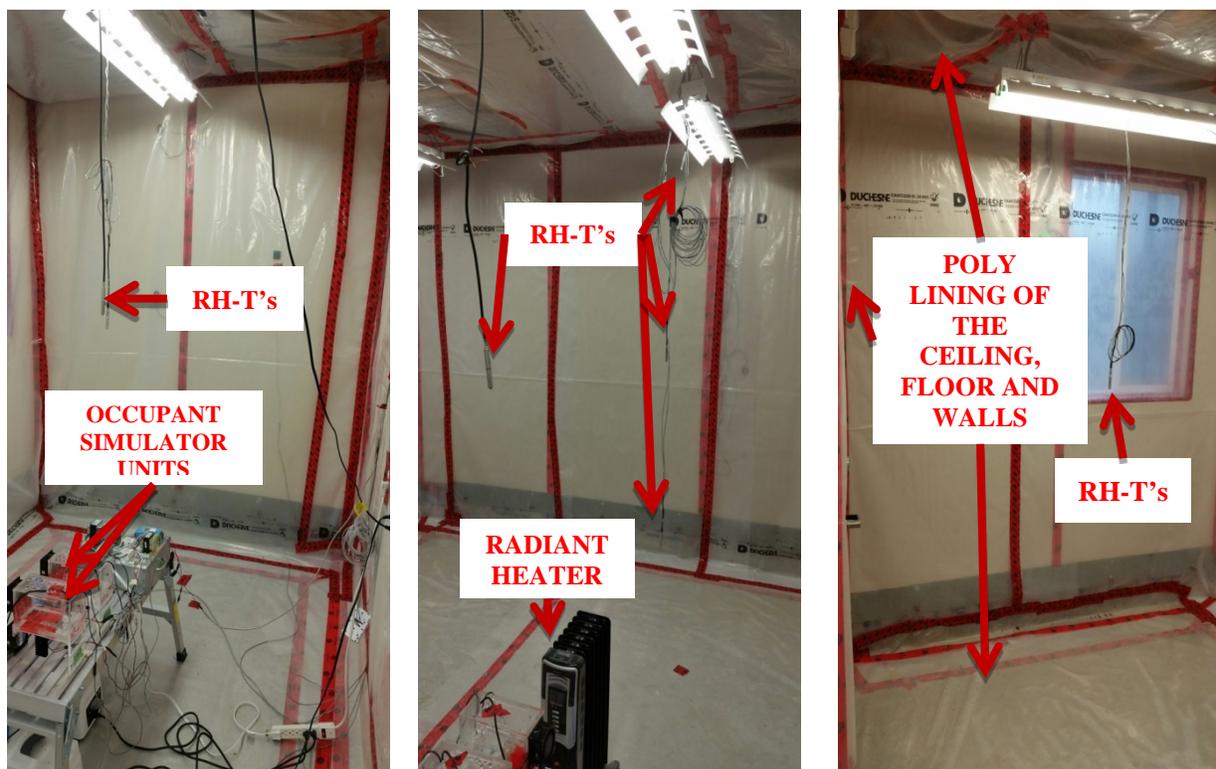

Figure 9 - Experimental setup of the WBPRL for field verification of the moisture production rates of the occupancy simulators

4.2.3 Household activity Simulator

As stated earlier, the daily household moisture generation is simulated by the humidification system. Box 1111 and 2221 are assembled in the south building while box 3112 and 4222 are assembled in the north building. The humidification systems are centrally positioned in the test facilities as in Figure 9 to ensure even distribution of the moisture being released in the test space. The even distribution of the test facility is facilitated by a ceiling fan to enhance air circulation by means of the increased convective air mixing. The pump is configured to operate continuously as triggered by the float sensor. The humidifier boxes are filled with water to the earlier marked height at which the pump comes on. This is setup this way so that the water height in the humidifier box remains constant throughout the experiment and the mass change of the water content of the water reservoir; which is the amount of water required to maintain the water height at a constant in the humidifier box, is regarded as the amount of moisture being put out by the humidification system into the test space. The initial weight of the water containers is weighed and documented.

The humidification system is autonomously controlled by means of a logic written in Vee that requires the user to input an excel sheet from which the hourly operation intervals are determined. The hourly operation intervals are derived from the moisture production rate profiles and the evaporation rate of the nebulizers. The moisture production rates per hour were derived from monitoring a household of four for a period of a year [34]. Over the monitoring period, the indoor and outdoor conditions were recorded including the temperature and the relative humidity. From the data recorded, psychrometric calculations were performed to derive the daily moisture production profiles. The daily moisture production profiles are statistically analyzed to determine the typical daily moisture production which corresponds to the 50th percentile normal distribution

and high moisture emission days which corresponds to the 95th percentile normal distribution [34]. Figure 10 shows the derived profile from the monitored suite data.
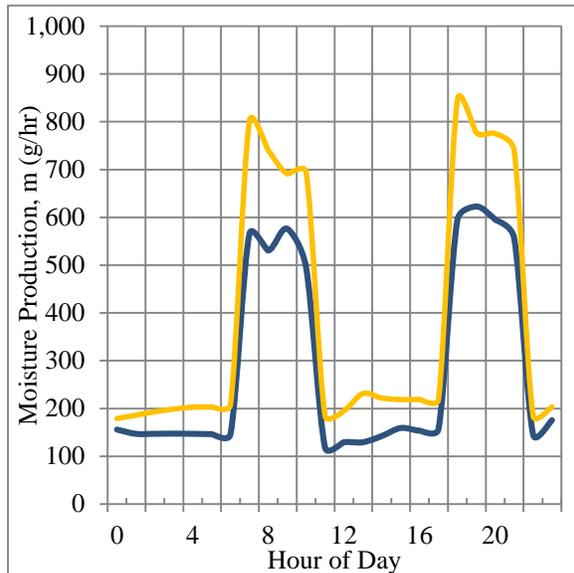
Figure 10 - Typical and high moisture production profiles from the monitored suite [34]
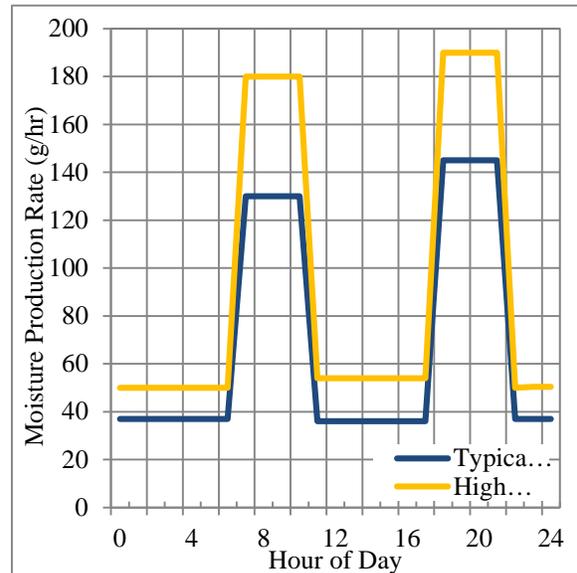
Figure 11 - Typical and high moisture production profiles used in the field experiment [34]

Considering the significant difference between the actual monitored suite and the test facility, the moisture production profile is scaled down based on the ratio of the occupiable floor area of the test buildings to that of the monitored apartment suite. To be more specific, the actual moisture production profiles used in the field experiment was scaled down by an amount of 75% (Figure 11).

4.2.4 Building Operation

Both buildings are equipped with radiant heaters that are configured to maintain the indoor temperature at 21°C while the HVAC system is configured to supply 100% fresh air that is neither heated nor cooled at a rate of 10cfm. The 21°C set-point is borne out of the typical comfort range in the colder periods according to ASHRAE and the ventilation rate is derived from the minimum

16

rate for ventilation as per ASHRAE 62.2 which is 7.5cfm per person plus 3cfm per 100 square foot.

4.3 Results

In this section, the results from the verification process are presented. The approach taken was to first verify the moisture production in one building before matching the humidity profile with that of the other building. The north building is designated the control building in this case.

Based on monitoring the family home earlier mentioned, the scaled down daily moisture production is 1.685kg. From monitoring and tuning the building, the humidification system generates the required amount of moisture to within 3%. To be precise, the daily moisture production of the humidification system is 1.629kg. This number was derived by weighing the water containers before and after a test run which is equivalent to a full day of operation (Table 2).

Table 2 - Measured daily moisture production of humidification system

NORTH BUILDING	
$Weight_{initial}$ [kg]	25.69
$Weight_{final}$ [kg]	24.061
ΔW [kg]	1.629

Further, the interior conditions of both buildings are harmonized. Figure 12 shows a comparison of the indoor air temperature in the north and south building. It can be seen that the indoor air temperature in both building sits below the set-point temperature which indicates that the radiant heaters are not capable of maintaining the indoor air temperature at the desired set-point with the

influx of the untempered outdoor air that is being introduced to the test space by means of the ventilation system. More important is the agreement between both indoor temperature profiles. To be specific, the maximum deviation registered for both indoor temperature profiles is 0.25°C, which is within measurable tolerance as per the specifications of the RH-T's; hence, it is concluded that there is no measurable difference between both test facilities. As such, the relative humidity can be used as a basis of comparison of the humidity levels in both facilities. Figure 12 shows a comparison of the relative humidity profile in the north and south building.
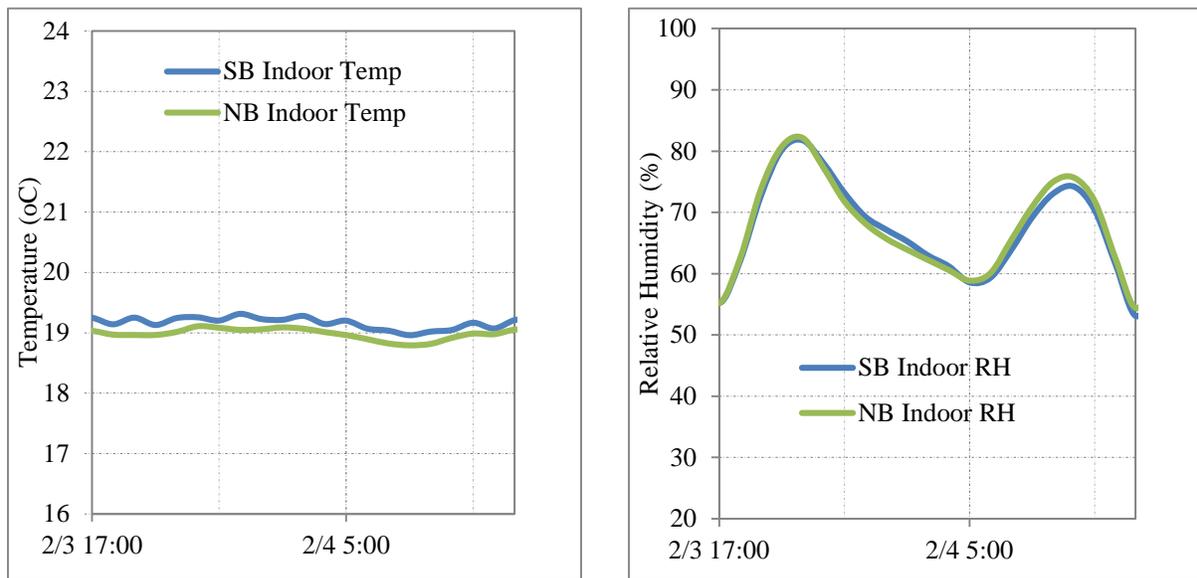
Figure 12 - Field verification of the moisture production rate in the north and south building: Indoor air temperature (L) and Relative humidity (R) comparison

As observed in Figure 12 above, the relative humidity profiles in both test facilities match to a reasonable degree. To be more specific, the maximum deviation recorded between the relative humidity profiles in both test facilities is 2%, which is within measurable tolerance as per the manufacturer specification of the RH-T's; hence, it can be concluded that there is no measurable difference between the relative humidity profiles in both test facilities.

4.3.1 Conclusion

It can clearly be seen that both buildings show very similar behavior when the interior conditions are compared. As well, the humidification system has been fine tuned to put out the correct amount of daily household moisture generation. In essence, experiments can proceed with confidence that the difference in humidity profiles experienced from here on is attributed to the difference in moisture buffering capabilities of the interior finishes. It should be noted that the actual evaporation rate of the nebulizer varied from the derived evaporation rate during the calibration phase. To be more specific, up to 30% deviation of the actual to the real evaporation rate is realized. Table 3 compares the calibrated evaporation rate to the actual evaporation rate. The discrepancy in both is attributed to the difference in the mode of operation used during calibration versus the actual. In the calibration, the operation mode is continuous whereas in the actual operation mode is intermittent. Hence, the evaporation rate derived during the calibration is the stable evaporation rate while that experienced in the actual operating mode is unstable since the system barely reaches equilibrium in most cases before it is turned off.

Table 3 - Comparison of the calibrated and actual moisture production rate

Box #	1111	2221	3112	4222
Calibrated Rate [g/hr]	90	141	70	126
Actual Rate [g/hr]	120	189	102	185

5 FIELD TESTING OF THE MOISTURE BUFFERING POTENTIAL OF MAGNESIUM OXIDE BOARD

Once the moisture production rate of the occupant simulators have been verified in both buildings, the field testing to investigate the moisture buffering potential of magnesia board commences.
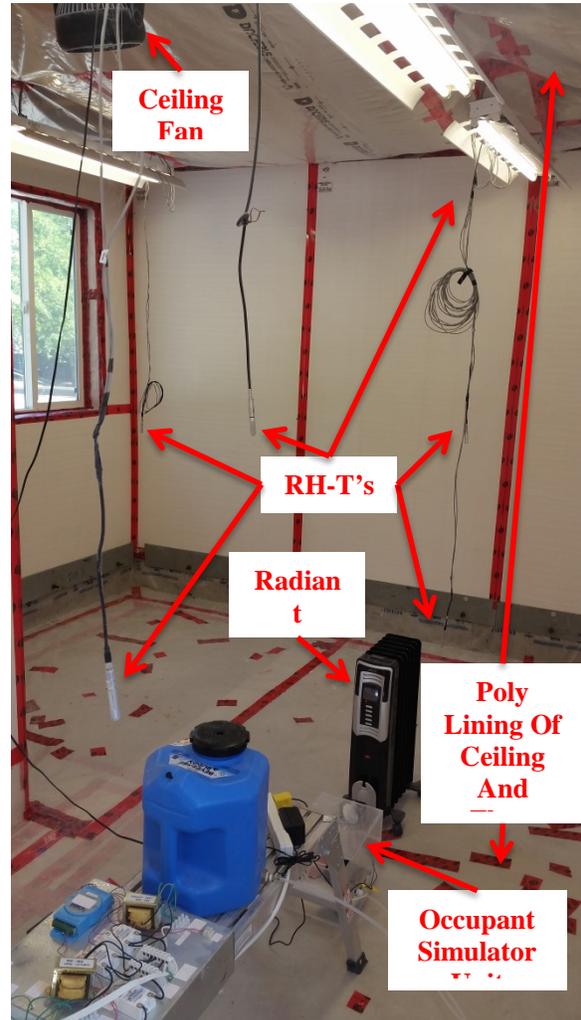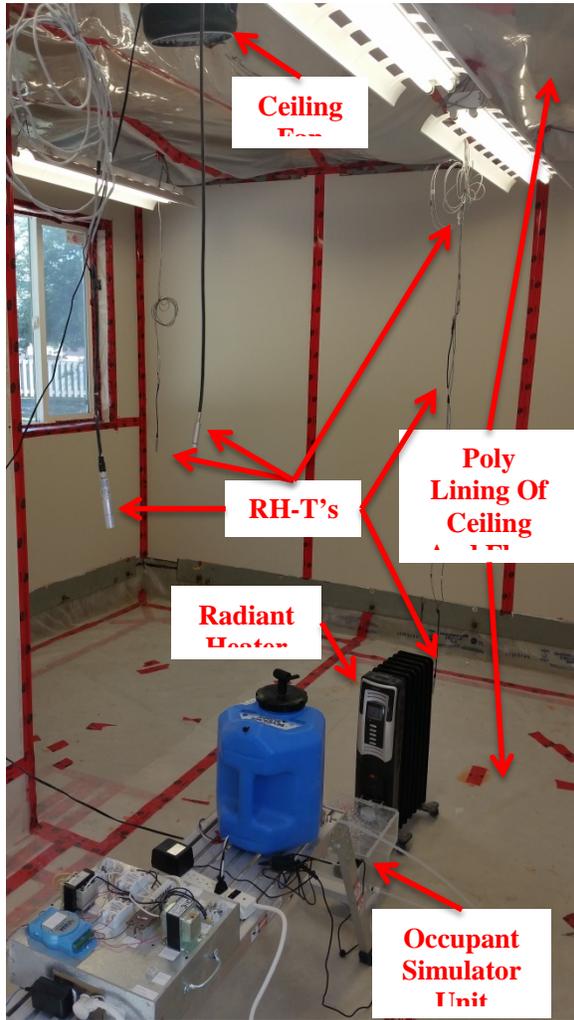

Figure 13 - North Building: Gypsum Board   **Figure 14 - South Building: MAGO Board**

As stated earlier, one the building is designated the "reference building" and the other the "test building". The north building is set as the "reference building" in which the gypsum interior finish (Figure 13) is installed for comparison purposes. The south building is setup to be the "test

building" in which the magnesium oxide board is installed (Figure 14). Initially, both boards are coated with two layers of primer sealer and 2 layers of paint to mimic industry practice as-built condition (Case I). Ideally, only a single primer sealer coat layer is required; however, because the initial coat of the primer still allowed for some visible pore spots on the magnesium oxide board, a second coat of primer sealer is applied. To ensure consistency in both buildings, the same is done to the gypsum board. The paint used is "BEHR Marque Interior Eggshell Enamel" and is regarded as one of the two popular interior paints at home depot. Secondly, both boards with no primer or paint are investigated to assess the impact of the surface coating i.e. the paint on the moisture buffering capability of both boards (Case II). Thirdly, the magnesia board is coated with a high permeance paint; its as-built condition and compared against gypsum without any surface coating (Case III). Lastly, both boards are compared under as-built conditions such that the magnesia board is coated with a high permeance paint and the gypsum is coated with BEHR latex paint earlier mentioned (Case IV).

To ensure that any difference in indoor behavior is attributed to the difference in material properties of both interior finishes, a few further considerations are taken into account during the experimental setup. Firstly, the surface area cover for both interior finishes is made to be near identical as much as possible. Secondly, the floor and ceiling is covered with polyethylene since they are a different material than the interior finishes. Thirdly, since the polyethylene layering of the ceiling is dropped down such that it adjoins the interior wall boards just to its starting edge from the top, discrepancies in the actual test space volume is almost inevitable. However, care is taken to ensure that both test spaces are of the same volume. Lastly, the integrity of the interfaces of the polyethylene seal as well as that on the ground that is prone to defects as a result of walking

is double checked and repaired before the commencement of any tests. With the experimental setup complete, four test runs are conducted and are detailed in the following section.

5.1 Test Runs

Four test runs are conducted to evaluate the moisture buffering potential of magnesia board. The four different conditions are come about by varying the hygrothermal loading and the ventilation rate. In the first case, both boards are exposed to typical moisture production and a ventilation rate of 15 cfm. This test case depicts conditions experienced in a newly constructed home where the moisture exposure is moderate and the ventilation meets the minimum ASHRAE requirement which specifies about 15cfm per person. However, in older houses that have deteriorated over time, there is no assurance that the ventilation requirement is being met. In extreme cases, there is little to no ventilation provided for the occupants. To simulate this case, the ventilation rate of 15cfm provided in the initial test run is halved. In order words, for this test condition, both wall boards are exposed to normal moisture production and a ventilation rate of 7.5 cfm. In the third case, both test facilities are exposed to high moisture production and a ventilation rate of 15cfm. The analogy behind this test case is a situation of over population of some homes with inadequate ventilation provided. In such cases, there is a higher potential for moisture accumulation and consequently envelope degradation through mold growth. It should be noted that the high moisture production case is derived as 1.5 times the typical or normal moisture production. In the fourth test case, both interior boards exposed to normal moisture production and the ventilation rate is relative humidity controlled. In this case, the relative humidity is maintained between 50% and 60% by modulating the ventilation rate between 0 cfm and 20 cfm such that if the relative humidity is less than 50% the ventilation is turned off and if the relative humidity is higher than 60%, the ventilation is operated at the maximum rate which is 20 cfm. Otherwise, if the relative humidity is

22

between 50% and 60%, the ventilation rate is modulated by linearly interpolating between 0 cfm and 20 cfm. It should be noted that the maximum ventilation rate; 20 cfm, in this test case is arbitrarily chosen between 15 cfm and 30 cfm. This is because, ventilating at the rate of 15 cfm is insufficient to maintain the relative humidity within the desired range. As well, ventilating at the rate of 30 cfm proved overly sufficient to maintain the relative humidity within the desired range. The idea behind the formulation of this test case is the added benefit of energy conservation as a result of moisture buffering. If any difference is seen, it should reflect in the reduction in the ventilation rate required at peak conditions. For the purpose of clarity the four test cases that were conducted are:

1. Typical moisture production and ventilation rate of 15 cfm

2. Typical moisture production and ventilation rate of 7.5 cfm

3. High moisture production and ventilation rate of 15 cfm

4. Typical moisture production and relative humidity controlled ventilation rate

5.2 Results

In this section, the results from the four test runs are presented and discussed. The moisture buffering capabilities of both materials is assessed using the relative humidity plots for both facilities. It should be noted that the indoor air temperature plots are not presented because the similarity in the indoor air temperature has been validated in the previous section. Also, the occupancy simulator systems are designed to introduce moisture into the space without altering the spatial air temperature distribution in the facility, hence, it is concluded that the variable of higher significance is the relative humidity.

5.2.1 Test Run #1 – Normal moisture production and ventilation rate of 15 cfm

Case I
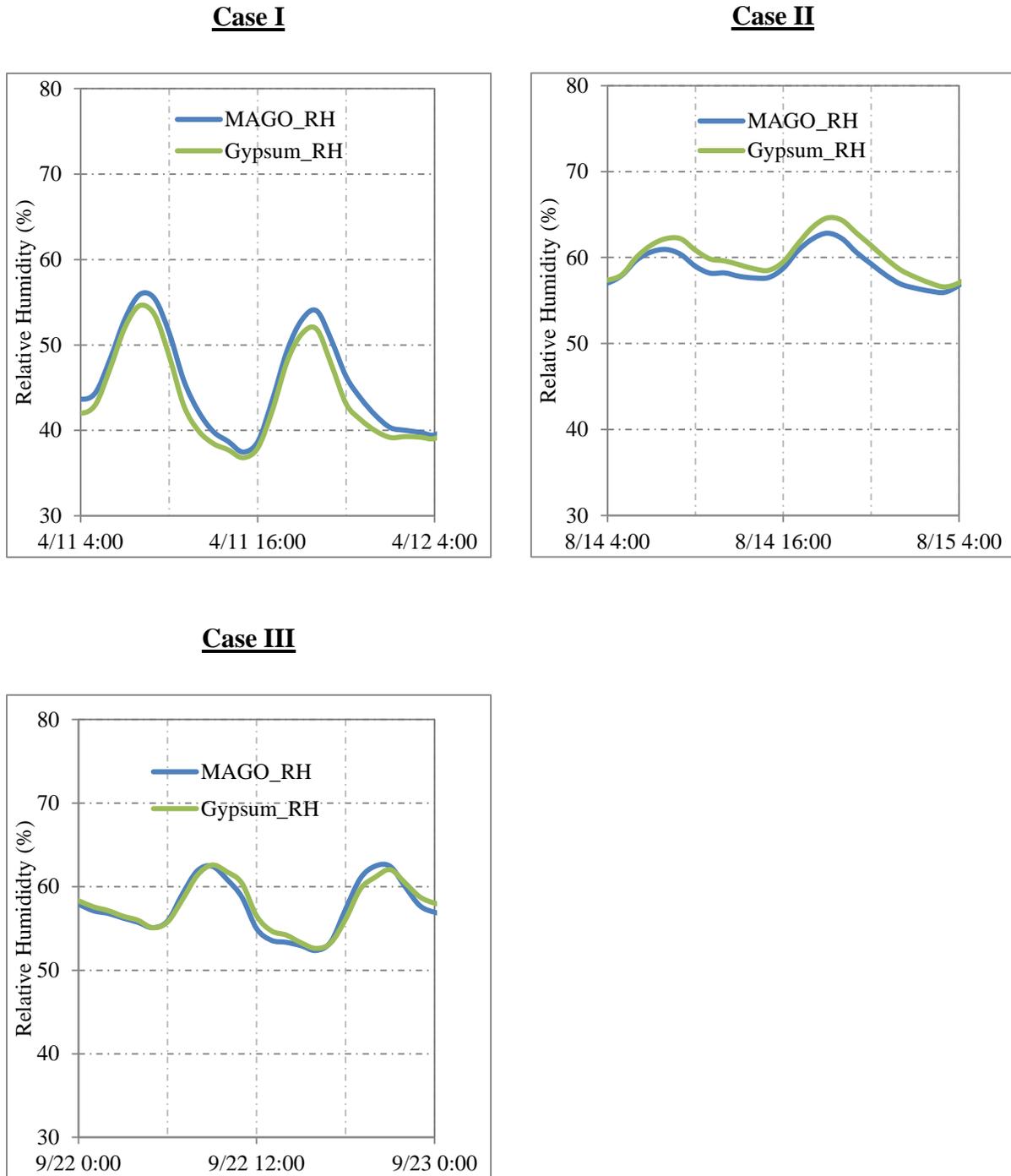
Case II

Case III

Figure 15 - Relative humidity comparison of both buildings exposed to normal moisture production and normal ventilation rate: (a) Case I (b) Case II (c) Case III

As stated earlier, this test run depicts the idea of relatively new buildings. Figure 15a compares an excerpt of the relative humidity in the north and south building for Case I. It should be noted that the excerpt presented in the figure below represents the behavior at stabilized conditions.

As can be observed there is a general trend of higher moisture in the morning and early evening which coincides with the period of elevated household activities when more moisture is released. As well, the relative humidity profile is typical of what is experienced in buildings, 40% at stable conditions and 60% when there is moisture production from occupants and their related activities. More important is the deviation of the relative humidity in both test facilities from each other. The maximum deviation calculated is 3.3% over the course of the experiment; however, the average deviation over the course of the experiment is 1.8%. Considering that the deviations are within tolerance limits, it is concluded that there is no measurable difference between both relative humidity profiles. Hence, the slight difference cannot be attributed to the moisture buffering of either of the interior finishes. Further, the similarity of slopes at relative humidity peaks and troughs suggest similar moisture buffering capabilities.

The impact of the paint on the moisture buffering capabilities of both boards can be seen in **Figure 15**b for case II. In both cases, the relative humidity fluctuation is damped. This is reflected in the relative humidity amplitude analysis in both figures which yields about 18% and 8.5% for the Case I and Case II respectively. This is about 50% reduction in the relative humidity amplitude owing to the cyclical moisture storage and release process that has the potential to stabilize the relative humidity in the space. Additionally, the temperature fluctuation in the test space under summer conditions also affects the relative humidity since the temperature is indirectly proportional to the relative humidity. Comparing the relative humidity profiles for Case II, one can observe some discrepancies between the two in that the relative humidity evolution in the test facility finished

with gypsum sits higher that in the test facility with magnesia board. A statistical analysis yields an average deviation of 1.2% and a maximum deviation of 2.3%, all within tolerance limits of the RH-T device. Hence, the moisture buffering capability of magnesium oxide board and gypsum are very comparable for test Case II.

In Case III, the impact of the high permeance paint on the moisture buffering capability of the magnesia boards is analyzed. Figure 15c compares the relative humidity profiles in both rooms. One can notice the higher relative humidity fluctuation compared to Case II for the same surface condition. This is due to the seasonal difference under which both tests were conducted. The present fall condition provides a more stable indoor air condition which amplifies the moisture fluctuation in the space. More important is the comparison of both relative humidity evolutions for which a slight difference is observed. To be specific, the average deviation between the two profiles is 0.67% while the max recorded for the day under study is 1.66%, all within tolerance limits of the relative humidity measuring device, hence, it is concluded that under these test conditions the high permeance paint does not significantly alter the moisture buffering capabilities of the magnesia board.

For Case IV, the data collected over the experiment period showed that the fluctuations did not stabilize after a week and a half of testing. Typically, at the onset of each experiment, there is significant offset between the relative humidity profiles. The room finished with magnesia board being the lower of the two. This is attributed to the higher porosity of the magnesia board. Upon saturation of the magnesia board, the moisture absorption rate is slowed and eventually but relative humidity profiles meet. Relative humidity profile evolutions beyond the point of encounter are regarded as stable behavior. However, in this case, both curves converge but the jump in interior air temperature attribute to uncontrollable outdoor weather conditions thereby drying out the

boards and pushing the saturation a few days ahead. This happened twice over the course of the experiment which further delayed stabilization.

5.2.2 Test Run #2 – Normal moisture production and ventilation rate of 7.5 cfm

By reducing the ventilation rate, it is anticipated that more moisture is accumulated in both facilities which may amplify the moisture buffering potential. Figure 16a compares the relative humidity plots in the two test spaces exposed to typical moisture production and low ventilation rate. As expected, there is higher moisture accumulation and is reflected in the higher levels of humidity observed compared to Run #1. In fact the relative humidity fluctuates between 50% and 70%, a 10% increase in peak relative humidity from the previous test run. More importantly, the maximum deviation calculated between both profiles is 1.4% while the calculated average deviation amounted to 0.6%. Both are within tolerance limits and the relative humidity profiles show similar slopes at relative humidity peaks and troughs; hence, the slight deviation cannot be attributed to the better moisture buffering of either of the interior finishes.

For Case II a different behavior is attained for both boards as expected (Figure 16b). It is worth noting that this test was conducted in typical summer conditions and a phase change material is installed in the test facility finished with the gypsum drywall. As such, the interior air temperature is significantly altered. In some cases, up to a 1°C difference between both temperature profiles is observed. Owing to the significant discrepancy, the relative humidity is recalculated using psychrometric relations with the temperature of the facility finished with magnesia board as the reference temperature. This is based on the assumption that, all things being equal the same temperature as in the south building is indicative of summer conditions. This may have introduced some irregularities in the results.

27
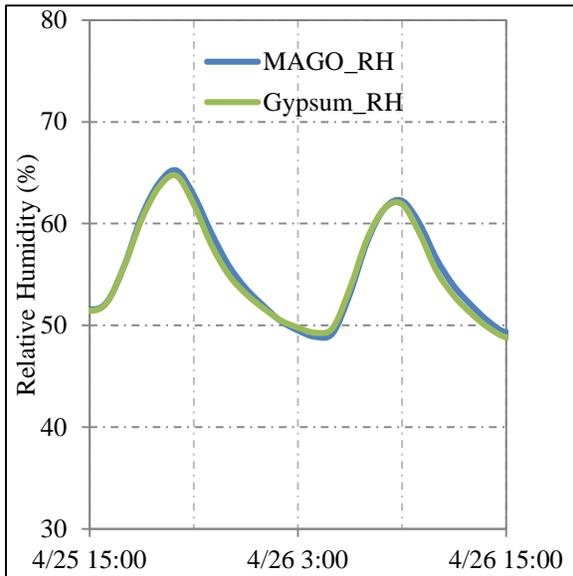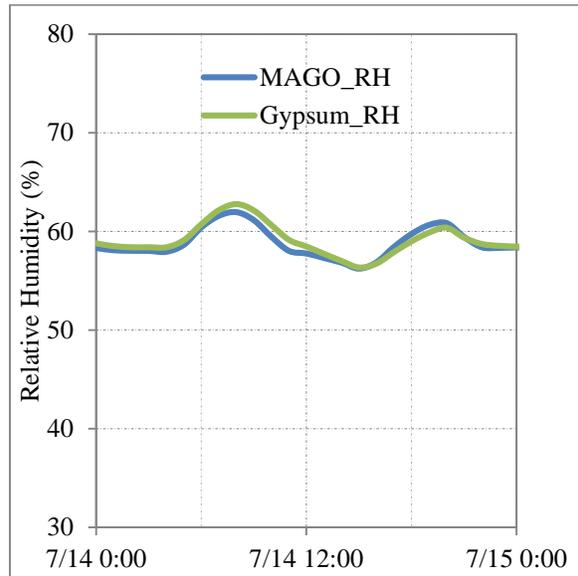
Case I

Case II

Case IV
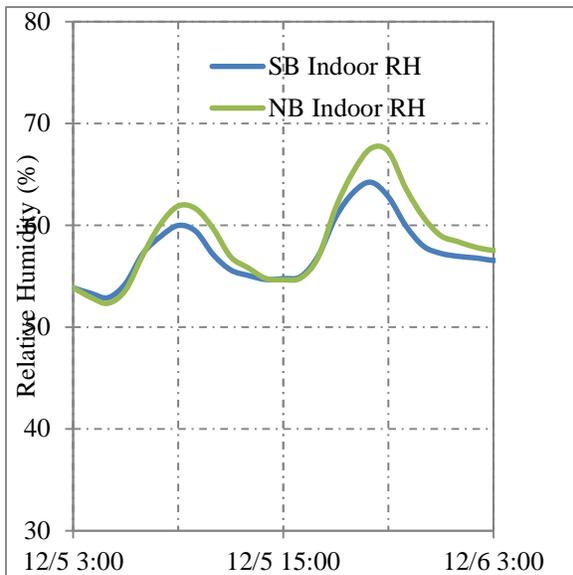
Figure 16 – Relative humidity of north and south buildings exposed to normal moisture production and low ventilation rate: (a) Case I (b) Case II (c) Case IV

As the case may be, the relative humidity amplitude is damped owing to the better surface porosity of the uncoated boards that facilitates efficient moisture release and storage. Putting it in numbers, the relative humidity amplitude without the paint is about 7.5% while that with the paint is 15%. This is a 50% reduction in the relative humidity amplitude. Further, the difference in the relative humidity profile evolutions between the two test facilities is analyzed. One can observe that the profiles are almost superimposed over each other which speaks to the similarity in the moisture buffering behavior between the two materials. To be specific, the maximum deviation of 1.0% and an average deviation of 0.4% between the two profiles is observed. Both are well within the tolerance limits of the RH-T's; hence, both materials exhibit similar moisture buffering capability for the test case and run under consideration.

In Case IV, a slightly better performance is observed in the room finished with the magnesia board (Figure 16c). This comes as no surprise because it is established in Run #1: Case III that the permeable paint on the magnesia board did not significantly affect the moisture buffering capability of the substrate. As can be seen in Figure 16d, the relative humidity peak is damped by up to 4.4% which is not within tolerance limits of the RH-T's, hence, the difference is attributed to the better porosity of the magnesia board surface treatment which allows for significant moisture storage and release. However, the increase in the trough temperature at moisture production downtimes is very small. To be specific, up to 0.6% trough relative humidity increase is realized. This is well within tolerance limits of the RH-T and can be effectively ignored. The insignificant trough relative humidity increase is attributed to the ineffectiveness of the ventilation in diluting the indoor moisture concentration following an event of high moisture.

5.2.3 Test Run #3 – High moisture production and ventilation rate of 15 cfm

This test run simulates high occupancy density in a home where the ASHRAE minimum ventilation requirement is not met as earlier mentioned.
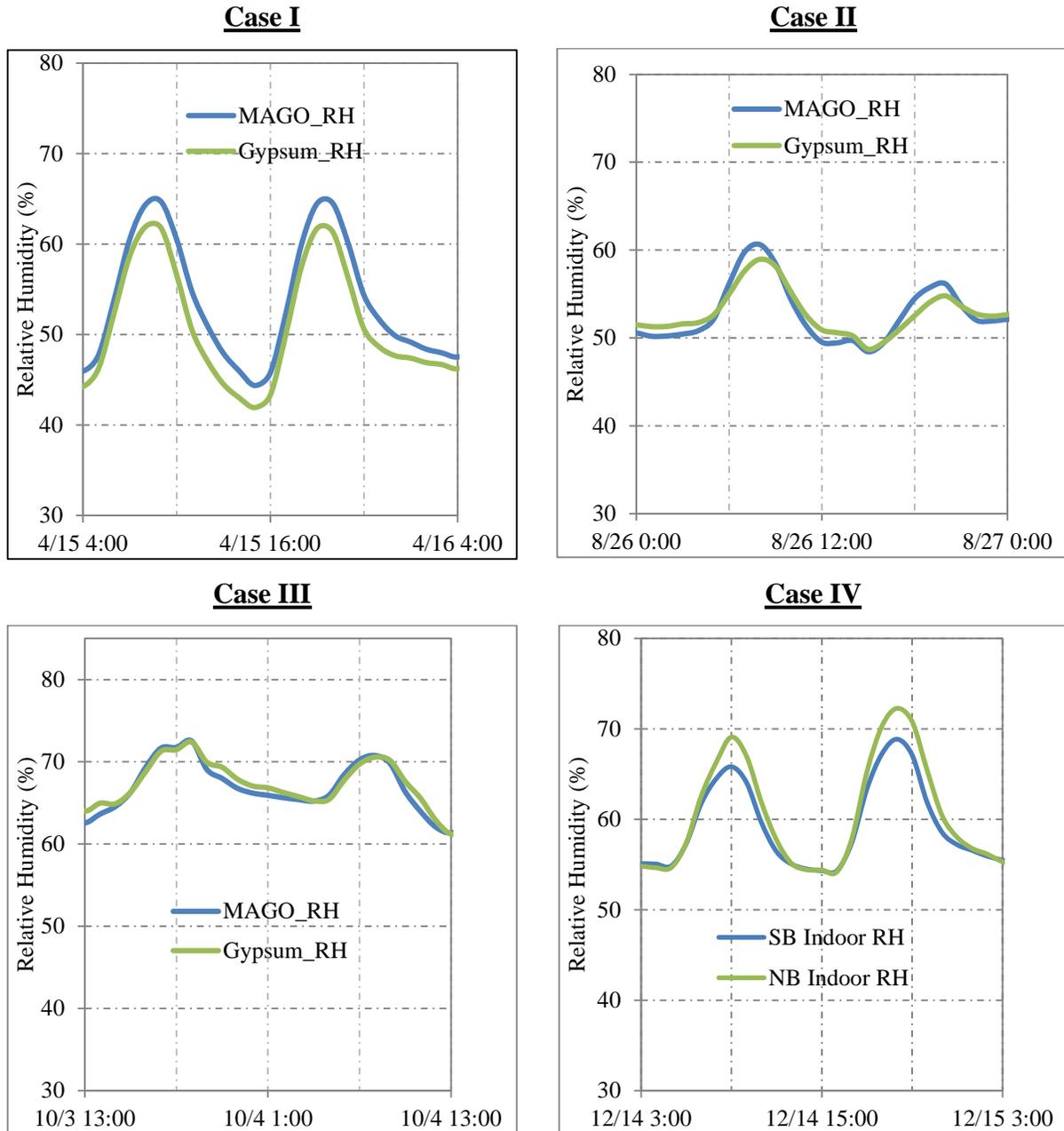

Figure 17 - Relative humidity comparison of both buildings exposed to high moisture production and normal ventilation rate: (a) Case I (b) Case II (c) Case III (d) Case IV

Figure 17a shows the relative humidity profiles in both test facilities for Case I. As can be seen in Figure 17a above, the relative humidity profile is similar to that of Run #2: Case I with respect to the moisture accumulation. More moisture is accumulated in the test facility and is reflected in the near 70% relative humidity at peak times. However, lower relative humidity values are achieved at moisture production downtimes owing to the higher ventilation rate that has a higher dilution effect on the moisture concentration in the test space. To be specific, the lowest relative humidity achieved in test Run #2: Case I is 50% compared to 41% achieved in the current case being discussed. By comparing the deviation of the both relative humidity profiles from each other, the direct offset of the relative humidity profiles can be observed. That of the test facility finished with magnesia board sits slightly higher than that in the test facility finished with gypsum. A statistical analysis yields a maximum deviation between the two profiles of 3.7% and an average deviation of 2.1%. At first thought, one may conclude that the maximum variation is not within tolerance of the RH-T's. However, the difference is amplified by the offset as opposed to the moisture buffering phenomenon. In other words, the relative humidity amplitude is very similar when compared to each other. As well, the slopes at relative humidity peaks and troughs are very similar. This further asserts the similarity in moisture buffering capability of the two

For Case II, the relative humidity amplitude is damped in both test facilities owing to the exposure of the surface porous structure that demonstrates better hygric properties (Figure 17b). To be specific, the relative humidity amplitude is damped from 25% to 12% which amounts to a halving of the relative humidity amplitude. More important is the slightly different moisture buffering characteristics exhibited by both materials which is evident in the relative humidity comparison. One can notice that the peak relative humidity in the test facility finished with gypsum is slightly lower than what is observed in the facility equipped with magnesia board. Consequently, the stored

up moisture is released at moisture production lows and is reflected in the higher relative humidity experienced in the facility finished with gypsum. Putting it in numbers, the gypsum wallboard lowers the peak relative humidity by up to 2.1% and increases the trough relative humidity by 1.4%. That being said, the peak reduction and the trough increase are within tolerance limits of the indoor relative humidity measuring device; hence, the moisture buffering characteristics of both materials are comparable.

For Figure 17c representative of case III, it is evident that the relative humidity amplitude is similar to case II. This is expected especially for the test facility finished with gypsum since both are tested with the same surface treatment. To be specific, the relative humidity amplitude calculated in both cases is 10%. One will also notice that despite the similar relative humidity amplitudes, the relative humidity profiles of case III are offset by about 10%. This is attributed to the different test periods in the year in that the moisture concentration in the ventilated air is uncontrollable varied. More important is the relative humidity profile evolutions in both test facilities. The near matching relative humidity profiles in both test facilities is observed with deviations in some instances. In fact, a statistical analysis shows that the maximum variation between both relative humidity profiles is 1.6% between peaks and 0.7% between troughs. Both are within tolerance limits of the RH-T pointing to comparable moisture buffering capabilities.

Further, Case IV shows damping of the relative humidity peaks in the test facility treated with the painted magnesia board (Figure 17d). Again, this comes as no surprise because the paint is permeable compared to the moisture closed latex paint. To be specific, up to 3.8% reduction in peak relative humidity is observed. Owing to the limited ability of the ventilation to dilute the moisture concentration in the space, the trough relative humidity does not dip low enough to warrant effective discharge of the stored up moisture. In fact, only a 0.4% increase is observed at

best. Of course, this is within tolerance limits of the RH-T, hence, this is equivalent to no improvement at low moisture production times.

5.2.4 Test Run #4 – Normal moisture production and RH controlled ventilation

One aspect of moisture buffering is the modulation of the relative humidity in the space, the other aspect of moisture buffering is the energy savings as a result of the moisture buffering especially when the ventilation is relative humidity controlled. In this case, the relative humidity is fixed between the range of 50% and 60% and any significant difference in the ventilation rate is attributed to the energy saving potential.

Figure 18 shows the relative humidity in both test facilities. It can clearly be seen that in both test facilities the relative humidity stays between 50% and 60% as suggested earlier on, which proves the ability of the ventilation to accurately moderate the relative humidity in the space. There is slight deviation between the two relative humidity profiles. In fact, up to 2.3% maximum deviation is calculated while an average deviation of 0.5% is recorded. Considering that both the maximum and average deviation between the two profiles calculated is within measurable tolerance of the RH-T's used, it is concluded that there is no measurable difference between the two profiles.
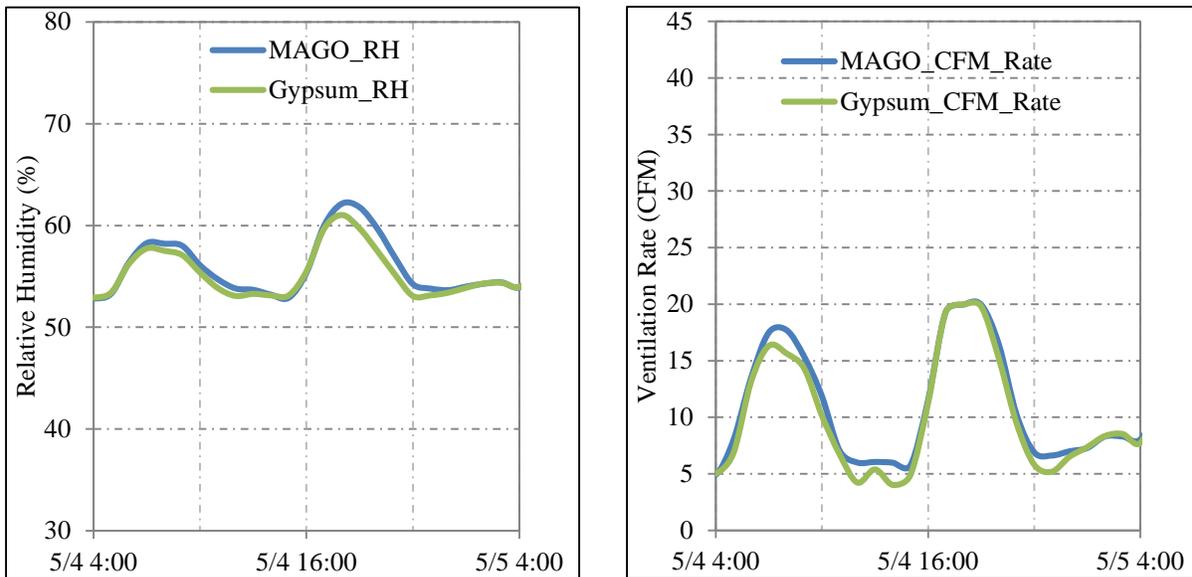
Figure 18 - Relative humidity (L) and Ventilation rate (R) comparison of both buildings exposed to normal moisture production and relative humidity controlled ventilation rate (Painted)

More important in this section is the relative ventilation requirements in the two test facilities; this is measured by the difference in ventilation rates between the two buildings. Figure 18 shows the ventilation rate per hour in both test facilities. As can be seen there is a close match in both profiles. This is expected because the relative humidity profiles aforementioned showed little to no measurable difference. Hence, it is concluded that there is no added benefit of energy savings attributed to the moisture buffering capability of either of the interior finishes over the other.

With both boards stripped off their surface treatment (no coating) while still maintaining the relative humidity in the test facility relatively between 50% and 60% as in Figure 19 a slightly different behavior is observed. One can observe in Figure 19 that the ventilation rate fluctuates between 10 cfm and 20 cfm as opposed to 5 cfm and 20 cfm in the previous case. This is attributed to the difference in time period during which the experiment is conducted. In the summer, the

moisture concentration in the outdoor air is higher thereby imposing a higher relative humidity at low moisture production times. Considering the ventilation rate is directly linked with the relative humidity in the space, the ventilation rate is higher as well. More important is the ventilation energy consumption comparison between the two test facilities, which is represented here by the ventilation rate in Figure 19. As can be seen, there is close match between both profiles suggesting a very similar ventilation energy requirements. This is expected because it was established in the previous test cases that gypsum showed similar moisture buffering capability to that of the magnesium oxide board interior finish. The similarity in the ventilation energy requirements may be as a result of the similarity in the moisture buffering capability of both materials. This is further explained below:
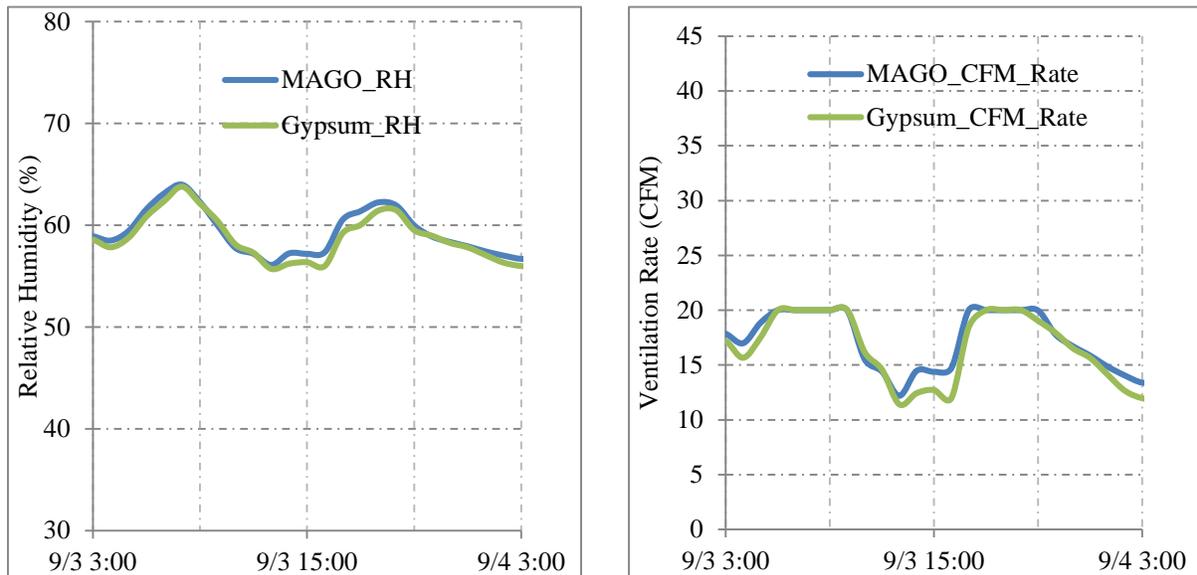
Figure 19 - Relative humidity (L) and Ventilation rate (R) comparison of both buildings exposed to normal moisture production and relative humidity controlled ventilation rate (Unpainted)

As shown in Figure 17b, by reason of the slightly better but comparable moisture buffering capability of the gypsum wallboard, the relative humidity peaks are lower and the relative humidity

troughs are higher. This should be the case with the ventilation rate considering the direct relationship. However, the lower ventilation rates at moisture production peaks cause the moisture concentration to increase in the space thereby increasing the relative humidity and the ventilation rate eventually increases. This can be said about the relative humidity troughs, at low peak production times, the relative humidity should be higher by reason of the stored up moisture at peak production times. Consequently, the ventilation rates are higher thereby reducing the moisture concentration in the test building. This also reduces the ventilation rate.

5.2.5 Discussion

The results from four tests runs that were conducted to compare the moisture buffering capacity of gypsum and magnesium oxide board were earlier presented. For the first three test runs different moisture production schemes were tested and the effect of surface treatment was analyzed. It was found in all three test runs that the latex paint on both boards rendered the boards near non-hygroscopic behavior in that the surface porosity was altered and limited effective storage and dissipation of moisture occur. To put it in perspective, the permeability of uncoated gypsum board according to ASHRAE Hand Book of Fundamentals chapter 26 is about 50 perms, but when finished with one coat of primer and 2 coats of paint, the permeance drops to about 10 perms which falls under the category of a class II vapor retarder. In fact, for the experimental setup, two primer coats were applied which may have the effect of further reducing the permeability of the boards. With the latex paint substituted for a permeable paint a different behavior is observed. The tests showed that it is possible to reap the moisture buffering benefits with the permeable paint when compared with a baseline building with gypsum board finished with a commonly used latex paint. Knowing that the surface treatment of these boards can mar the moisture buffering capacity of these boards it is therefore necessary to employ finishes that do not significantly alter the surface

36

porosity of the boards. In general, the experimental results suggest that the moisture buffering potential of magnesia board is comparable with that of gypsum board.

In the fourth run, the energy benefits in terms of ventilation energy savings as a result of moisture buffering were exploited. The ventilation scheme was such that the relative humidity was maintained between 50 % and 60% while linearly interpolating between ventilation OFF and 20cfm. It was found that this ventilation scheme did not exploit the moisture buffering capacity of both materials in the sense that the moisture build up in the test space counteracted the reduced ventilation rate as a result of the moisture buffering.

6 CONCLUSION/SUMMARY

Indoor relative humidity control is very important because if it accumulates in excess it can lead to building envelope failures. Also, this excess humidity creates a favorable environment for mold growth which is risky for the respiratory health. Indoor humidity is typically controlled by ventilation, however, this has negative impacts on the energy performance of the building in that providing ventilation beyond the minimum requirements as stated by building codes consumes more energy. Moisture buffering provides a passive means to control the humidity in the zone. As such, the ventilation requirement is reduced. The humidity control as a result of this moisture buffering phenomenon varies for different materials, as some material have shown to have a better moisture buffering potential over the other. That of Magnesium oxide board is not known and was investigated in this project.

This investigation was carried out in the field, such that two test facilities were monitored. One was regarded as the "reference building" and the other as the "test building". The reference building was finished with gypsum as a basis of comparison because it is the most frequently used

interior finish in the industry, while the test building was finished with magnesium oxide board. Both interior finish boards were tested under typical moisture production profiles which were developed by monitoring the household activities for a family of four for a period of a year and statistically deriving the average daily moisture production profile. The profiles were then scaled down as per the ratio of the volume of the BCIT test facility to the monitored home. The moisture production profile was simulated by an autonomously controlled humidification system that consisted of a humidification box; housing the mist maker and the fan, the pump and the water reservoir.

The moisture generation of this humidification system was first calibrated and verified to within 3% of the actual moisture generation required. As well, both the interior conditions of the reference building and test building was verified to within 1.4% of each other. Upon, verification of the humidification system and validation of the test facilities, four tests were conducted. The tests were: (1) Normal moisture production and 15 cfm, which was defined to simulate a newly built home with minimum ventilation requirements being met, (2) Normal moisture production and 7.5 cfm, which was designed to simulate an old home were the ventilation requirements is not being met, (3) High moisture production and 15 cfm, which was designed to simulate a home with high occupancy density, and (4) Normal moisture production and relative humidity controlled ventilation rate, which was designed to investigate the energy saving potential as a result of moisture buffering. The relative humidity profiles in all four cases were compared and the moisture buffering potential was analyzed for four distinct surface treatments: Case I - Both boards covered with latex paint, Case II – Both boards uncoated, Case III – Magnesia board covered with permeable paint and gypsum uncoated, and Case IV – Magnesia board coated with permeable paint and gypsum with latex paint.

From the analysis, it was found that in the first test run, the average deviation between the two humidity profiles over the course of the experiment was 1.8% for Case I, 1.2% for Case II and 0.67% for case III. In the second test run, the deviation between the two humidity profiles were 0.6% for Case I, 0.4% for Case II and 4.4% for case IV. In the third test run, the average deviation between the two humidity profiles over the course of the experiment was 2.1% for Case I, 1.4% for Case II, 1.6% for case III, and 3.8% for Case IV. From discrepancies calculated for Case I's and Case II's for the first three test runs, it was concluded that the latex paint significantly altered the moisture buffering characteristics of both substrates both gypsum and magnesia board show similar moisture buffering characteristics. For all discrepancies calculated for Case III, it was concluded that with the magnesia board covered with the permeable paint, the moisture buffering capabilities of the material was not significantly altered. The results in test #4 indicate that for the ventilation scheme considered in this study there is no added benefit of energy savings attributed to the moisture buffering capability of either of the interior finishes over the other.

That being said, considering that both materials displayed similar moisture buffering capabilities, the surface condition of magnesia board renders it a more favorable material in that it is not susceptible to mold growth compared to the paper facing of the gypsum wallboard.

7 REFERENCES

[1]   Clarke, J. A., Johnstone, C. M., Kelly, N. J., McLean, R. C., Rowan, N. J., & Smith, J.
       E. (1999). A technique for the prediction of the conditions leading to mould growth in
       buildings. *Building and Environment*, *34*(4), 515-521.

[2]   Isaksson, T., Thelandersson, S., Ekstrand-Tobin, A., & Johansson, P. (2010). Critical

conditions for onset of mould growth under varying climate conditions. *Building and*

environment, *45*(7), 1712-1721.

[3]   Johansson, P., Bok, G., & Ekstrand-Tobin, A. (2013). The effect of cyclic moisture and

temperature on mould growth on wood compared to steady state conditions. *Building*

and Environment, *65*, 178-184.

[4]   Johansson, P., Svensson, T., & Ekstrand-Tobin, A. (2013). Validation of critical

moisture conditions for mould growth on building materials. *Building and Environment*,

62, 201-209.

[5]   Zhang, H., & Yoshino, H. (2010). Analysis of indoor humidity environment in Chinese

residential buildings. *Building and Environment*, *45*(10), 2132-2140.

[6]   Mlakar, J., & Štrancar, J. (2013). Temperature and humidity profiles in passive-house

building blocks. *Building and Environment*, *60*, 185-193.

[7]   Woloszyn, M., Kalamees, T., Abadie, M. O., Steeman, M., & Kalagasidis, A. S. (2009).

The effect of combining a relative-humidity-sensitive ventilation system with the

moisture-buffering capacity of materials on indoor climate and energy efficiency of

buildings. *Building and Environment*, *44*(3), 515-524.

[8]   what does the scientific literature tell us about the ventilation-health relationship in

public and residential buildings

[9]   Rahim, M., Douzane, O., Le, A. T., Promis, G., Laidoudi, B., Crigny, A., ... & Langlet, T. (2015). Characterization of flax lime and hemp lime concretes: Hygric properties and moisture buffer capacity. *Energy and Buildings*, *88*, 91-99.

[10]   Collet, F., Chamoin, J., Pretot, S., & Lanos, C. (2013). Comparison of the hygric behavior of three hemp concretes. *Energy and Buildings*, *62*, 294-303.

[11]   McGregor, F., Heath, A., Fodde, E., & Shea, A. (2014). Conditions affecting the moisture buffering measurement performed on compressed earth blocks. *Building and Environment*, *75*, 11-18.

[12]   Orosa, J. A., & Baaliña, A. (2009). Improving PAQ and comfort conditions in Spanish office buildings with passive climate control. *Building and environment*, *44*(3), 502-508.

[13]   Ge, H., Yang, X., Fazio, P., & Rao, J. (2014). Influence of moisture load profiles on moisture buffering potential and moisture residuals of three groups of hygroscopic materials. *Building and Environment*, *81*, 162-171.

[14]   Ghali, K., Katanani, O., & Al-Hindi, M. (2011). Modeling the effect of hygroscopic curtains on relative humidity for spaces air conditioned by DX split air conditioning system. *Energy and Buildings*, *43*(9), 2093-2100.

[15]   Yoshino, H., Mitamura, T., & Hasegawa, K. (2009). Moisture buffering and effect of ventilation rate and volume rate of hygrothermal materials in a single room under steady state exterior conditions. *Building and environment*, *44*(7), 1418-1425.

[16] Rode, C., & Grau, K. (2008). Moisture buffering and its consequence in whole building hygrothermal modeling. *Journal of Building physics*, *31*(4), 333-360.

[17] Hameury, S. (2005). Moisture buffering capacity of heavy timber structures directly exposed to an indoor climate: a numerical study. *Building and Environment*, *40*(10), 1400-1412.

[18] Cerolini, S., D'Orazio, M., Di Perna, C., & Stazi, A. (2009). Moisture buffering capacity of highly absorbing materials. *Energy and Buildings*, *41*(2), 164-168.

[19] Osanyintola, O. F., & Simonson, C. J. (2006). Moisture buffering capacity of hygroscopic building materials: experimental facilities and energy impact. *Energy and Buildings*, *38*(10), 1270-1282.

[20] Gómez, I., Guths, S., Souza, R., Millan, J. A., Martín, K., & Sala, J. M. (2011). Moisture buffering performance of a new pozolanic ceramic material: Influence of the film layer resistance. *Energy and Buildings*, *43*(4), 873-878.

[21] Abadie, M. O., & Mendonça, K. C. (2009). Moisture performance of building materials: From material characterization to building simulation using the Moisture Buffer Value concept. *Building and Environment*, *44*(2), 388-401.

[22] Orosa, J. A., & Oliveira, A. C. (2009). Energy saving with passive climate control methods in Spanish office buildings. *Energy and Buildings*, *41*(8), 823-828.

[23] Casey, S. P., Hall, M. R., Tsang, S. C. E., & Khan, M. A. (2013). Energetic and hygrothermal analysis of a nano-structured material for rapid-response humidity buffering in closed environments. *Building and Environment*, *60*, 24-36.

[24] Allinson, D., & Hall, M. (2010). Hygrothermal analysis of a stabilised rammed earth test building in the UK. *Energy and Buildings*, *42*(6), 845-852.

[25] Liuzzi, S., Hall, M. R., Stefanizzi, P., & Casey, S. P. (2013). Hygrothermal behavior and relative humidity buffering of unfired and hydrated lime-stabilised clay composites in a Mediterranean climate. *Building and Environment*, *61*, 82-92.

[26] Wang, Y., Liu, Y., Wang, D., & Liu, J. (2014). Effect of the night ventilation rate on the indoor environment and air-conditioning load while considering wall inner surface moisture transfer. *Energy and Buildings*, *80*, 366-374.

[27] Le, A. T., Maalouf, C., Mai, T. H., Wurtz, E., & Collet, F. (2010). Transient hygrothermal behavior of a hemp concrete building envelope. *Energy and buildings*, *42*(10), 1797-1806.

[28] Evrard, A., & De Herde, A. (2009). Hygrothermal performance of lime-hemp wall assemblies. *Journal of building physics*.

[29] Barclay, M., Holcroft, N., & Shea, A. D. (2014). Methods to determine whole building hygrothermal performance of hemp–lime buildings. *Building and Environment*, *80*, 204-212.

[30] Orosa, J. A., & Oliveira, A. C. (2011). Reducing energy peak consumption with passive climate control methods. *Energy and Buildings*, *43*(9), 2282-2288.

[31] Evrard, A., & De Herde, A. (2009). Hygrothermal performance of lime-hemp wall assemblies. *Journal of building physics*.

[32] Dubois, S., Evrard, A., & Lebeau, F. (2013). Modeling the hygrothermal behavior of biobased construction materials. *Journal of Building Physics*, 1744259113489810.

[33] Tariku, F. et al. (2013). Development of a Whole-Building Performance Research Laboratory for Energy, Indoor Environment and Building Envelope Durability Study.

[34] Pedram, S., & Tariku, F. (2015). Determination of Representative Daily Moisture Production Profile for Energy and Durability Performance Assessment of Residential Buildings.